Nomogram to predict the presence of PSMA-negative but FDG-positive lesion in castration-resistant prostate cancer: a multicenter cohort study

Ther Adv Med Oncol

2024, Vol. 16: 1–13

DOI: 10.1177/17588359231220506

Jian Pan*, Tingwei Zhang*, Shouzhen Chen*, Ting Bu*, Jinou Zhao*, Xudong Ni, Benkang Shi, Hualei Gan, Yu Wei, Qifeng Wang, Beihe Wang, Junlong Wu, Shaoli Song, Feng Wang, Chang Liu, Dingwei Ye and Yao Zhu

Abstract

Background: PSMA-negative but FDG-positive (PSMA–/FDG+) lesion in dual-tracer (^{68}Ga-PSMA and ^{18}F-FDG) positron emission tomography/computed tomography (PET/CT) is associated with an unfavorable response to Lutetium-177 (^{177}Lu)-PSMA-617. This study sought to develop both radiomics and clinical models for the precise prediction of the presence of PSMA–/FDG+ lesions in patients with castration-resistant prostate cancer (CPRC).

Methods: A cohort of 298 patients who underwent dual-tracer PET/CT with a less than 5-day interval was included. The evaluation of the prognostic performance of the radiomics model drew upon the survival data derived from 40 patients with CRPC treated with ^{177}Lu-PSMA-617 in an external cohort. Two endpoints were evaluated: (a) prostate-specific antigen (PSA) response rate, defined as a reduction exceeding 50% from baseline and (b) overall survival (OS), measured from the initiation of ^{177}Lu-PSMA-617 to death from any cause.

Results: PSMA–/FDG+ lesions were identified in 56 (18.8%) CRPC patients. Both radiomics (area under the curve [AUC], 0.83) and clinical models (AUC, 0.78) demonstrated robust performance in PSMA–/FDG+ lesion prediction. Decision curve analysis revealed that the radiomics model yielded a net benefit over the 'screen all' strategy at a threshold probability of ⩾4%. At a 5% probability threshold, the radiomics model facilitated a 21% reduction in ^{18}F-FDG PET/CT scans while only missing 2% of PSMA–/FDG+ cases. Patients with a low estimated score exhibited significantly prolonged OS (hazard ratio = 0.49, $p = 0.029$) and a higher PSA response rate (75% *versus* 35%, $p = 0.011$) compared to those with a high estimated score.

Conclusion: This study successfully developed two models with accurate estimations of the risk associated with PSMA–/FDG+ lesions in CRPC patients. These models held potential utility in aiding the selection of candidates for ^{177}Lu-PSMA-617 treatment and guiding ^{68}Ga-PSMA PET/CT-directed radiotherapy.

Plain language summary

Predictive nomogram for PSMA-/FDG+ lesion

This study developed two models with accurate estimations of the risk associated with specific lesions in prostate cancer.

Correspondence to:
Dingwei Ye
Yao Zhu
Department of Urology, Fudan University Shanghai Cancer Center, Shanghai, China

Shanghai Genitourinary Cancer Institute, Shanghai, China

Department of Oncology, Shanghai Medical College, Fudan University, Shanghai, China
dwye.shca@gmail.com
zhuyao@fudan.edu.cn

Shaoli Song
Chang Liu
Department of Oncology, Shanghai Medical College, Fudan University, Shanghai, China

Department of Nuclear Medicine, Fudan University Shanghai Cancer Center, Shanghai, China
shaoli-song@163.com
lcggtt@163.com

Feng Wang
Department of Nuclear Medicine, Nanjing First Hospital, Nanjing Medical University, Nanjing, China
fengwangcn@hotmail.com

Jian Pan
Tingwei Zhang
Jinou Zhao
Xudong Ni
Yu Wei
Beihe Wang
Junlong Wu
Department of Urology, Fudan University Shanghai Cancer Center, Shanghai, China

Shanghai Genitourinary Cancer Institute, Shanghai, China

Department of Oncology, Shanghai Medical College, Fudan University, Shanghai, China

Shouzhen Chen
Benkang Shi
Department of Urology, Qilu Hospital, Cheeloo College of Medicine, Shandong University, Shandong Province, China

Ting Bu
Department of Nuclear Medicine, Nanjing First Hospital, Nanjing Medical University, Nanjing, China

Department of Nuclear Medicine, The Affiliated Jiangning Hospital with Nanjing Medical University, Nanjing, China

Hualei Gan
Qifeng Wang
Department of Oncology, Shanghai Medical College, Fudan University, Shanghai, China

Department of Pathology, Fudan University Shanghai Cancer Center, Shanghai, China

*These authors contributed equally

Keywords: CRPC, FDG, nomogram, PSMA

Received: 16 May 2023; revised manuscript accepted: 21 November 2023.

Introduction

Metastatic castration-resistant prostate cancer (mCRPC) remains incurable despite significant advancements in diverse drug regimens. The emergence of prostate-specific membrane antigen (PSMA) as a theragnostic agent with heightened expression in mCRPC lesions has revolutionized mCRPC management.[1–4] Lutetium-177 (^{177}Lu) PSMA-617 is a radiolabeled small-molecule inhibitor that binds with high affinity to PSMA and delivers β particle radiation. The success of the VISION and TheraP trial has established the antitumor activity and favorable safety profile of ^{177}Lu-PSMA-617 in men with mCRPC.[1,2] A pivotal criterion for radioligand therapy (RLT) in both trials is the manifestation of high PSMA expression within the tumor, as determined by discernible tracer uptake on ^{68}Ga-PSMA positron emission tomography/computed tomography (PET/CT) scans.[5] However, the substantial heterogeneity of metastases in prostate cancer (PCa), particularly in advanced mCRPC with de-differentiation, poses a challenge.[6,7] Advanced disease exhibits reduced PSMA expression, leading to limited or absent uptake on ^{68}Ga-PSMA PET/CT. This subset of patients experiences discordance between ^{68}Ga-PSMA and ^{18}F-fluorodeoxyglucose [FDG] PET/CT imaging, indicative of a more aggressive phenotype with suboptimal responses to PSMA-directed therapies.[8–11] The TheraP trial, in contrast to the VISION trial, implemented additional ^{18}F-FDG PET/CT scanning to identify and exclude patients with FDG-positive but PSMA-negative (PSMA−/FDG+) lesions, resulting in the exclusion of 18% (52/291) of patients.[1,2] Furthermore, the augmented assessment of tumor burden afforded by supplemental ^{18}F-FDG PET/CT scans holds significant implications in the selection of candidates for metastases-directed stereotactic body radiotherapy (SBRT).[12,13]

The identification of patients at risk of discordant lesions in ^{68}Ga-PSMA and ^{18}F-FDG (dual-tracer) PET/CT represents a crucial advancement, contributing to enhanced precision in treatment strategies and a reduction in unnecessary costs.[8,9,14] In light of this, our research endeavored to develop PSMA−/FDG+ lesion prediction nomograms, grounded in clinical data and ^{68}Ga-PSMA-11 PET/CT tumor characteristics. The predictive efficacy of these nomograms will be systematically compared with the Renji model, the sole reported PSMA−/FDG+ lesion prediction model, employing dichotomized thresholding of Gleason score (GS; 8) and prostate-specific antigen (PSA; 7.9 ng/ml) to categorize patients into distinct risk groups.[15] In addition, we assessed the survival impact of the radiomics nomogram using an external cohort.

Methods

Study design and participants

Between April 2019 and January 2022, patients with CRPC who underwent dual-tracer PET/CT at two academic hospitals (Fudan University Shanghai Cancer Center, Shanghai, and Qilu Hospital, Shandong) were retrospectively assessed for eligibility based on predefined criteria. Inclusion criteria encompassed histological confirmation of prostate adenocarcinoma and the availability of a comprehensive medical record. Exclusion criteria included the presence of active malignancies other than PCa, histologic features indicative of pure neuroendocrine or small-cell cancer, and prior ^{177}Lu-PSMA-617 treatment. CRPC was defined according to the European Association of Urology guidelines.[16] Ethical approval was obtained from the institutional ethics committees of both institutes, aligning with the Declaration of Helsinki. Informed consent requirements were waived due to the retrospective nature of the study. The reporting of this study conformed to the reporting recommendations for tumor marker prognostic studies.[17]

PET/CT imaging and image analysis

Radiotracers were administered on different days with an interval of fewer than 5 days. For ^{18}F-FDG PET/CT, patients fasted for at least 6 h. The blood glucose levels before the injection of the tracer should be lower than 10 mmol/L. Routine scans commenced 60 min post-tracer administration (3.7 MBq/kg). ^{68}Ga-PSMA-11 PET/CT did not necessitate fasting, with patients

ingesting 500 mL of water during a 2-h period before acquisition (2.0 MBq/kg) without dietary preparation. A 60-min interval was also adopted for uptake time. PET/CT scans were performed using a Siemens mCT Flow PET/CT scanner (Siemens Healthcare, Knoxville, TN, USA). A non-contrast-enhanced CT scan was performed using the following parameters: slice thickness of 3 mm, increment of 2 mm, and soft tissue reconstruction kernel, 120 keV. Immediately after CT scanning, a whole-body PET (from the level of the skull base to the knee) was acquired in 3D (matrix 200×200). A multimodality computer platform (Syngo; Siemens Healthcare) was used for image review and manipulation. Transaxial, coronal, and sagittal reconstructions of CT, PET, and fusion PET/CT data for interpretation can be produced by this system.

All scans were visually evaluated independently by three blinded nuclear medicine specialists with at least 5-year experience in PET/CT reading. Any assessment results inconsistency was resolved by joint discussion. During visual interpretation, each reviewer marked regions of suspected disease based on a two-point scale: zero as negative and one as positive. The region was graded as one only when a visually positive lesion was found. Positive lymph nodes [LNs] were verified only if the ^{68}Ga-PSMA-11 or ^{18}F-FDG uptake was locally accumulated and higher than the blood pool (mediastinal blood pool). Positive visceral lesions were verified only if the ^{68}Ga-PSMA-11 or ^{18}F-FDG uptake was locally accumulated and higher than the background activity of the surrounding involved organ or region. Positive bone lesions were verified only if the ^{68}Ga-PSMA-11 or ^{18}F-FDG uptake was locally accumulated and higher than physiologic bone marrow. The uptake of a lesion was semi-quantitatively expressed as the maximum standardized uptake value (SUVmax). The PET/CT imaging interpretation at two academic hospitals followed these prespecified protocols.

Development of the prediction models

A clinically driven, evidence-based approach guided variable selection. First, a very recent literature review was used to identify significant predictors for the presence of PSMA−/FDG+ disease.[7] Second, three consensus meetings were organized with clinical experts including urologists (JP, TZ, SC, TB, JW, DY, and YZ), two expert uroradiologists (CL and SS), and two uropathologists (HG and QW). The principles of variable selection were usefulness, availability, and relevance. Finally, 17 variables were selected for model construction. Variables included clinical information [including baseline PSA value, GS, distant metastases at diagnosis, history of abiraterone/docetaxel treatment, albumin (ALB), alkaline phosphatase (ALP), alanine transaminase (ALT), aspartate aminotransferase (AST), total bilirubin (TBIL), and lactate dehydrogenase (LDH)] and ^{68}Ga-PSMA-11 PET/CT tumor characteristics [including the number of metastases, LN status, bone status, visceral status, SUVmax, and average SUV (SUVmean)]. Clinical laboratory assessments were done no more than 7 days before dual-tracer PET/CT.

Evaluation of the predictive performance of the models

The Akaike information criteria (AIC) determined the model with optimal discrimination, while the receiver operating characteristic curve (ROC) and area under the curve (AUC) gauged discrimination ability. Calibration curves were plotted *via* bootstrapping with 1000 resamples to assess the calibration of the developed models. Decision curve analysis (DCA) was conducted to estimate a net benefit for prediction models defined as the proportion of true positives minus the proportion of false positives.[18,19] The net benefit of the model at each threshold probability was estimated.

In addition, survival data of ^{177}Lu-PSMA-617-treated mCRPC patients with complete medical records from an external cohort (Nanjing cohort)[20] were utilized to evaluate the prognostic value of the radiomics model. Two endpoints were evaluated: (a) PSA response rate, defined as a reduction exceeding 50% from baseline[1] and (b) overall survival (OS), measured from the initiation of ^{177}Lu-PSMA-617 to death from any cause.

Statistical analyses

Image findings and baseline characteristics were collected, with continuous data presented as medians and interquartile range (IQR), and categorical data as frequencies and percentages. Categorical variables were compared using the chi-square test or Fisher exact test. Continuous variables were compared using Student's *t*-test or Mann–Whitney *U* test, when appropriate. Predictors of PSMA−/FDG+ lesion were identified through univariate logistic regression analysis, with variables ($p < 0.05$)

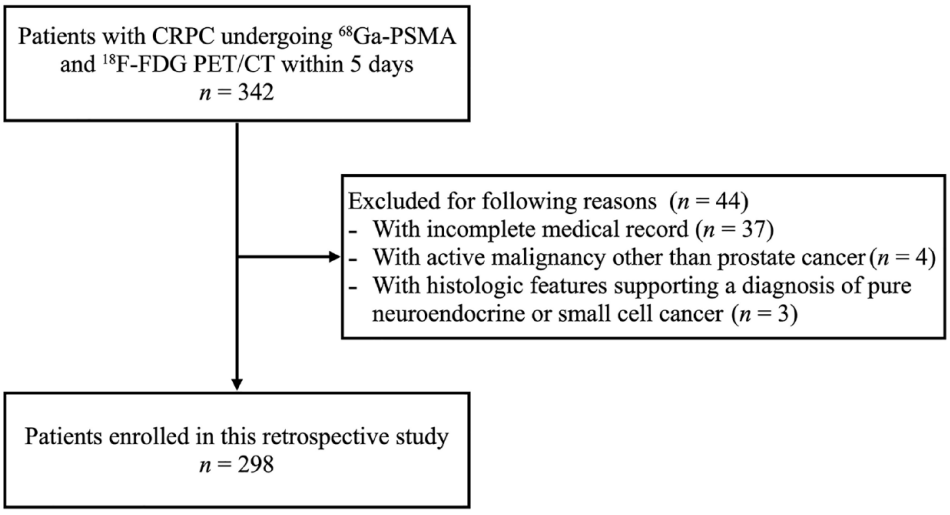

Figure 1. Study flowchart.
CRPC, castration-resistant prostate cancer; FDG, fluorodeoxyglucose; PSMA, prostate-specific membrane antigen.

included in stepwise multivariable logistic regression analysis. In addition, another two continuous parameters, SUVmax and SUVmean, were important reference indicators for selecting candidates for the ^{177}Lu-PSMA-617 treatment.[1,2,21] Thus, these two variables were included in the stepwise multivariable logistic regression analysis irrespective of the univariate analysis results. The Kaplan–Meier method was used to estimate OS outcomes. Hazard ratio (HR) and 95% confidence intervals (95% CI) were calculated. Statistical analyses were performed with R software (version 4.2.0; R Core Team, Vienna, Austraia).

Results

Metastases and heterogeneity detected by dual-tracer PET/CT

The workflow of our study design is outlined in Figure 1. A cohort of 298 patients with CRPC was incorporated into the study. The demographic and clinical characteristics of these patients are listed in Table 1 and Supplemental Table S1. The median age at the time of PET/CT was 68 (IQR, 63–73), with a corresponding median PSA level at enrollment was 2.5 (IQR, 1.1–8.0). Notably, 79.5% (237/298) presented with GS ⩾8 disease and 78.9% (235/298) exhibited PSMA-positive metastases.

A total of 117 PSMA−/FDG+ lesions were identified in 56 patients (Supplemental Table S2/S3). These lesions were distributed across node [29 (24.8%)], bone [83 (70.9%)], and visceral [5 (4.3%)]. Of the 56 patients, 15 (36.6%) had multiple PSMA−/FDG+ lesions. The validation of PSMA−/FDG+ lesions involved several procedures: histological analysis after salvage LN dissection or dual-tracer PET/CT-guided target biopsy (n = 3), follow-up ^{18}F-FDG PET/CT or conventional imaging confirmation (n = 108), or target radiation therapy with consecutive PSA declines of ⩽0.02 ng/ml (n = 6). Only one patient experienced interpretation discrepancy among three readers, attributed to a supraclavicular LN lesion with intense FDG uptake. A subsequent false-positive result was identified in this lesion following a tumor-free histopathological report post ^{18}F-FDG PET/CT-guided target biopsy.

Development of nomogram

Among the 17 evaluated variables, 11 met the criteria for variable selection, qualifying for multivariable analysis (Table 2). Two models emerged: the radiomics model [Figure 2(a)] integrating clinical data and ^{68}Ga-PSMA-11 PET/CT tumor characteristics, and the clinical model [Figure 2(b)] based solely on clinical variables. In the stepwise logistic regression analysis, the radiomics model, constructed by SUVmax, PSA, number of lesions, bone metastases, prior docetaxel therapy, and ALP, exhibited the lowest AIC value (224.13). Consequently, these six variables were selected for radiomics model construction and the subsequent generation of online calculator (https://peterjianfuscc.shinyapps.io/DynNomapp/). The radiomics

Table 1. Characteristics of the 298 patients in the study cohort.

Parameter	Result
Median age at baseline, years (IQR)	68 (63–73)
Median PSA at baseline, ng/ml (IQR)	2.5 (1.1–8.0)
Gleason score, *n* (%)	
⩽7	61 (20)
>7	237 (80)
Metastases site, *n* (%)	
LN	138 (46)
Bone	170 (57)
Visceral	14 (5)
Number of metastases, *n* (%)	
⩽5	201 (67)
>5	97 (33)
Prior treatment, *n* (%)	
Abiraterone	88 (30)
Docetaxel	57 (19)
Abiraterone and docetaxel	24 (8)
At least one PSMA–/FDG+ lesion, *n* (%)	56 (19)

FDG, fluorodeoxyglucose; LN, lymph node; PSA, prostate-specific antigen; PSMA, prostate-specific membrane antigen.

model displayed an AUC of 0.83 [95% CI: 0.77–0.89; Figure 3(a)], with calibration curves illustrating a commendable alignment between predicted and actual PSMA−/FDG+ lesion positivity (Supplemental Figure S1). The clinical model, constructed by PSA, prior docetaxel therapy, and ALP, yielded the lowest AIC value (233.34) and an AUC of 0.78 (95% CI: 0.70–0.86).

Model predictive performance analysis

Subsequently, the predictive capabilities of the developed nomograms were systematically evaluated in comparison with the established Renji model.[15] In our cohort, the Renji model exhibited a higher AIC value (269.36) compared to both the radiomics and clinical models, indicative of its inferior fit. Furthermore, the AUC value for the Renji model (0.67; 95% CI: 0.60–0.74) in our cohort was observed to be lower than that of both the radiomics and clinical models, underscoring its diminished discriminatory power. In DCA, both the radiomics and clinical models demonstrated a net benefit over either the 'screen all' strategy or the Renji model at threshold probabilities of ⩾4% and ⩾8%, respectively [Figure 3(b)]. The reduction in ^{18}F-FDG PET/CT and the rate of missing PSMA−/FDG+ lesions were detailed across various threshold probabilities derived from the radiomics and clinical models (Table 3). Encouragingly, with a 5% cutoff, the radiomics model avoided 21% (62/298) of unnecessary ^{18}F-FDG PET/CT scans while only missing 2% (1/56) of PSMA−/FDG+ cases. At a 10% probability threshold, the radiomics model averted 49% (145/298) of ^{18}F-FDG PET/CT scans while missing 16% (9/56) of PSMA−/FDG+ lesions. Conversely, using a 10% cutoff from the clinical model resulted in a 27% (15/56) omission of men with PSMA−/FDG+ lesions but spared 67% (201/298) of additional ^{18}F-FDG PET/CT scans.

Association between PSMA–/FDG+ lesion risk and survival outcome post ^{177}Lu-PSMA-617 treatment

The prognostic performance of the radiomics model was elucidated using a cohort of 40 eligible mCRPC patients from the Nanjing cohort (Table 4).[20] At baseline, the median age was 68 (IQR, 61–75), and the median PSA level at enrollment was 17.7 (IQR, 76.6–383.5). Remarkably, 92.5% (37/40) of patients presented with >5 PSMA-positive lesions, with 32.5% (13/40) having received prior docetaxel treatment.

The radiomics score was computed using the formula: radiomics score = 100 − 0.833 × SUVmax of ^{68}Ga-PSMA-11 PET/CT (continuous variable) + 0.055 × PSA value (continuous variable) + 21.659 × number of lesions (categorical variable) + 19.244 × bone metastases (categorical variable) + 28.520 × prior docetaxel treatment (categorical variable) + 37.145 × ALP value (categorical variable). Patients with >5 PSMA-positive lesions, bone metastases, prior docetaxel treatment, or ⩾ULK ALP value were assigned a value of 1, the rest of the patients were assigned a value of 0. With a median follow-up of 10.9 (IQR 7.6–16.2) months, 87.5% (35/40) of patients died and PSA response was achieved in 55.0% (22/40) of patients [Figure 4(a)]. In addition, in comparison to patients with ⩾median predicted scores, those with <median predicted score exhibited a

Table 2. Logistic regression model to predict the presence of PSMA−/FDG+ disease ($n = 298$).

Variable			Stepwise multivariable logistic regression analysis			
	Univariate analysis		Radiomics model		Clinical model	
	OR (95% CI)	*p*	OR (95% CI)	*p*	OR (95% CI)	*p*
Continuous PSA value	1.00 (1.00–1.01)	<0.01*	1.00 (1.00–1.01)	0.01	1.00 (1.00–1.01)	0.02
Continuous SUVmax value	1.00 (0.99–1.02)	0.51#	0.96 (0.94–0.99)	<0.01	–	–
Continuous SUVmean value	1.06 (0.97–1.15)	0.20#	–	–	–	–
Prior abiraterone treatment (Yes *versus* No)	1.90 (1.03–3.46)	0.04*	–	–	–	–
Prior docetaxel treatment (Yes *versus* No)	5.11 (2.69–9.75)	<0.001*	4.63 (2.18–9.98)	<0.001	5.13 (2.51–10.62)	<0.001
Gleason score (⩾8 *versus* <8)	3.14 (1.31–9.36)	0.02*	–	–	–	–
ALB value (⩾ULK *versus* <ULK)	0.80 (0.18–2.54)	0.73	–	–	–	–
ALP value (⩾ULK *versus* <ULK)	8.49 (4.28–17.14)	<0.001*	8.35 (3.57-20.39)	<0.001	8.55 (4.07-18.43)	<0.001
ALT value (⩾ULK *versus* <ULK)	1.22 (0.18–5.28)	0.80	–	–	–	–
AST value (⩾ULK *versus* <ULK)	2.63 (0.52–11.18)	0.20	–	–	–	–
TBIL value (⩾ULK *versus* <ULK)	0.74 (0.24–1.90)	0.57	–	–	–	–
LDH value (⩾ULK *versus* <ULK)	0.91 (0.32-2.27)	0.85	–	–	–	–
M1 at diagnosis (Yes *versus* No)	2.19 (1.22–4.02)	<0.01*	–	–	–	–
Number of metastases (>5 *versus* ⩽5)	4.39 (2.41–8.16)	<0.001*	2.56 (1.10–5.99)	0.03	–	–
With LN metastases (Yes *versus* No)	1.12 (0.62–2.00)	0.71	–	–	–	–
With bone metastases (Yes *versus* No)	3.00 (1.57–6.06)	<0.01*	2.54 (1.07–6.21)	0.04	–	–
With visceral metastases (Yes *versus* No)	3.51 (1.11–10.54)	0.03*	–	–	–	–

CI, confidence interval; FDG, fluorodeoxyglucose; LDH, lactate dehydrogenase; LN, lymph node; PSA, prostate-specific antigen; PSMA, prostate-specific membrane antigen; OR, odds ratio; SUV, standardized uptake value; TBIL, total bilirubin.
*A significant difference ($p \leqslant 0.05$).
#Included in stepwise multivariable logistic regression analysis regardless of univariate analysis results.

higher PSA response rate [75% *versus* 35%, $p = 0.011$; Figure 4(b)] and a significant prolonged OS [median 12.3 months *versus* 9.4 months; HR = 0.49, 95% CI = 0.25–0.97, $p = 0.029$; Figure 4(c)].

Discussion

In the context of a retrospective multicenter cohort, we crafted two nomograms to assess the risk of PSMA−/FDG+ disease in CRPC patients undergoing dual-tracer PET/CT. Notably, our radiomic model (AUC, 0.83) and clinical model (AUC, 0.78) showcased commendable efficacy, surpassing the antecedent model (AUC, 0.67).[15] Intriguingly, the probability of PSMA−/FDG+ disease exhibited a robust correlation with the PSA response rate and overall survival outcomes in patients with mCRPC subjected to ^{177}Lu-PSMA-617 treatment.[20]

Tumor heterogeneity emerges as a pivotal factor in treatment resistance and failure.[4] Patients scheduled for PSMA-directed therapy, including RLT and imaging-guided metastases radiation, often exhibit heterogeneity in tumor biology and prior treatments.[1,2,22,23] In a retrospective study, Kerstin *et al.* stratified mCRPC patients treated with ^{177}Lu-PSMA-617 according to the presence of PSMA−/FDG+ disease, revealing significantly

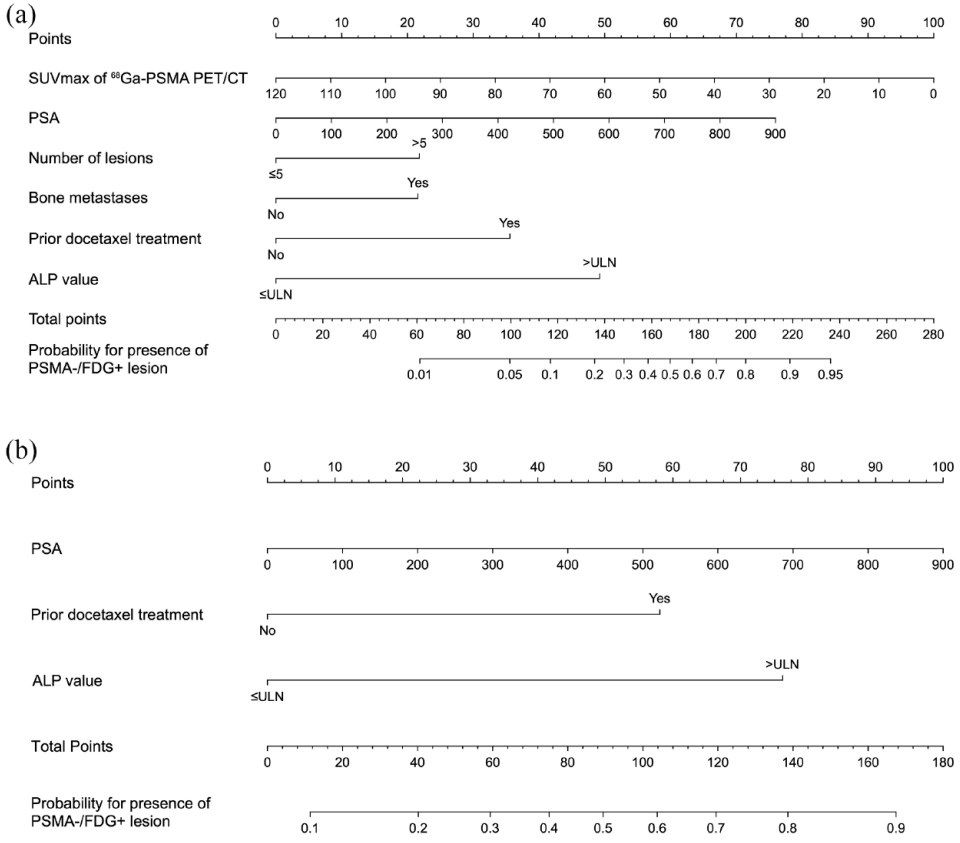

Figure 2. Radiomics model and clinical model. (a) A radiomics model with clinical variables and ^{68}Ga-PSMA PET/CT tumor characteristics incorporated. (b) Clinical model constructed based on clinical variables to predict the presence of PSMA−/FDG+ lesion.
FDG, fluorodeoxyglucose; PET/CT, positron emission tomography/computed tomography; PSA, prostate-specific antigen; PSMA, prostate-specific membrane antigen; SUV, standardized uptake value.

lower OS rates in those with PSMA−/FDG+ disease despite comparable clinical characteristics.[24] TheraP trial's exploratory analysis also highlighted the adverse impact of a high volume of ^{18}F-FDG avid tumors on survival, irrespective of treatment assignment.[25] The driver role of FDG-positive tumors in CRPC was in accordance with our survival analyses. In addition, radio-ablation of PSMA−/FDG+ lesions would improve the outcomes of the CRPC patients.[13] In a prospective cohort, Pan *et al.* reported that 23.0% of CRPC patients had PSMA−/FDG+ disease, and radio-ablation of all PSMA−/FDG+ lesions resulted in a high PSA response rate (86.2% of patients had a PSA decline ⩾90%) compared to historical cohorts.[13] Therefore, an accurate estimate of the risk of PSMA−/FDG+ lesions may improve the selection for additional ^{18}F-FDG PET/CT staging and subsequently optimize precision treatment with affordable cost.[26]

The investigation by Chen *et al.* elucidated that 23.2% of patients exhibiting PSA progression during androgen deprivation therapy harbored at least one PSMA−/FDG+ lesion, and these patients demonstrated higher PSA and GS levels according to the Renji model.[15] Our model exhibited commendable performance across a spectrum of threshold probabilities compared with Renji model. In addition, we discerned that docetaxel-refractory CRPC, prognostically linked to poor outcomes in ^{177}Lu-PSMA-617 treatment, was associated with a higher incidence of PSMA−/FDG+ disease.[21] The predictive value of some laboratory variables was evaluated. ALP, as a more bone-related parameter, demonstrated a robust correlation with the presence of PSMA−/FDG+ lesions. Interestingly, variable bone metastases also contributed to an augmented positivity for PSMA−/FDG+ lesions.[21,27] Hence, we posited that a deeper exploration of bone-related

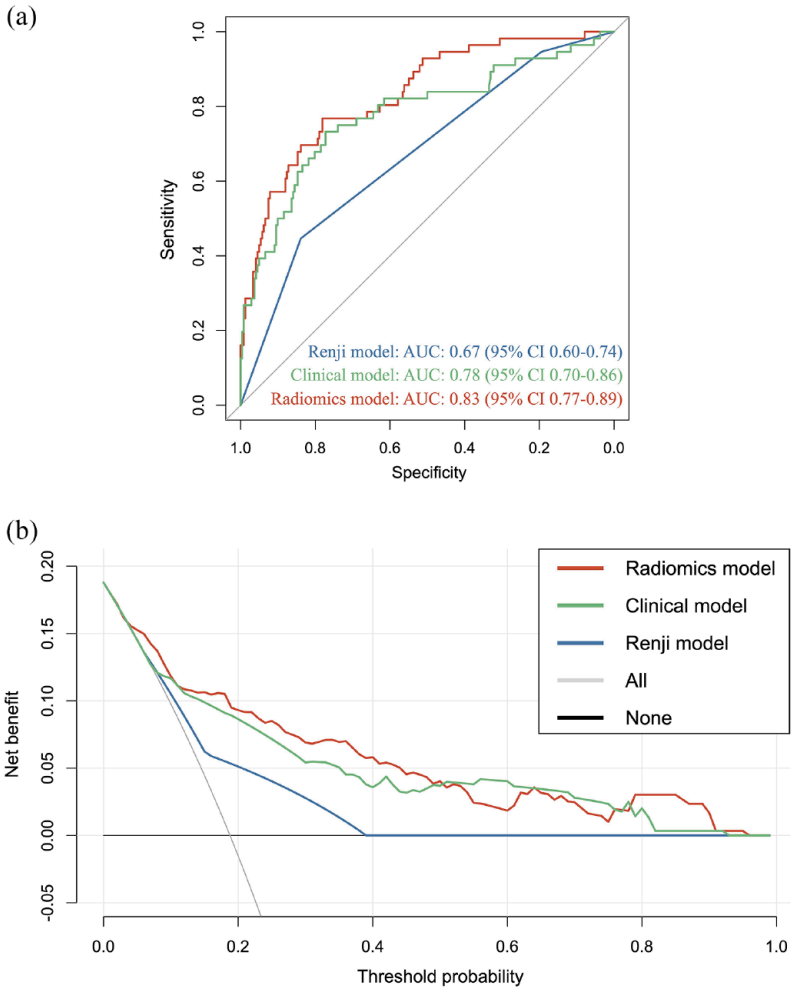

Figure 3. Performance of radiomics model and clinical model in PSMA−/FDG+ lesion predicting. (A) Comparison of ROC between the radiomics model, clinical model, and Renji model for the prediction of the presence of PSMA−/FDG+ lesion. (B) DCA of the radiomics model, clinical model, and Renji model for the prediction of PSMA−/FDG+ lesion.
DCA, decision curve analyses; FDG, fluorodeoxyglucose; PSMA, prostate-specific membrane antigen; ROC, receiver operating characteristic curve.

parameters was merited, given their potential as metrics for worsening disease under ^{177}Lu-PSMA-617 treatment. Furthermore, it was rational to consider SUVmax in ^{68}Ga-PSMA PET/CT as another imaging parameter associated with PSMA−/FDG+ lesions. This association was plausible as tumor PSMA expression may decrease or be lost during various lines of treatment, potentially leading to more conspicuous positive ^{18}F-FDG PET/CT findings.[7] These findings harmonized with the results in the multivariable survival analysis of ^{177}Lu-PSMA-617 treatment, where these three variables retained their status as independent prognostic factors for PSA progression-free survival.[21] This consistency underscored the potential translation of predictive imaging phenotypes in CRPC into judicious applications of PSMA-targeted RLT. For enhanced clinical applicability, we meticulously devised both radiomic and clinical nomograms, adaptable to both community and academic practice, serving as valuable screening tools for patient referral and strategic treatment sequence arrangements. For example, patients with a low probability of PSMA−/FDG+ disease may be more inclined to benefit from RLT, while those with a high probability may discuss clinical trials if available.

Table 3. Reduction in ^{18}F-FDG PET/CT and number of PSMA–/FDG+ lesions missing according to the threshold probabilities of 5%, 10%, 15%, 20%, and 25% derived from the radiomics model and clinical model in included patients with CRPC.

Probability threshold	^{18}F-FDG PET/CT		PSMA–/FDG+ lesion	
	Performed (%)	Avoided (%)	Found (%)	Missing (%)
Screen all	298 (100)	–	56 (100)	–
Radiomics model				
⩾5%	236 (79)	62 (21)	55 (98)	1 (2)
⩾10%	153 (51)	145 (49)	47 (84)	9 (16)
⩾15%	107 (36)	191 (64)	43 (77)	13 (23)
⩾20%	84 (28)	214 (72)	39 (70)	17 (30)
⩾25%	68 (23)	230 (77)	36 (64)	20 (36)
Clinical model				
⩾5%	298 (100)	0 (0)	56 (100)	0 (0)
⩾10%	97 (33)	201 (67)	41 (73)	15 (27)
⩾15%	93 (31)	205 (69)	39 (70)	17 (30)
⩾20%	92 (31)	206 (69)	39 (70)	17 (30)
⩾25%	92 (31)	206 (69)	39 (70)	17 (30)

CRPC, castration-resistant prostate cancer; FDG, fluorodeoxyglucose; PSMA, prostate-specific membrane antigen.

Table 4. Characteristics of the ^{177}Lu-PSMA-617-treated patients from the Nanjing cohort, $n = 40$.

Characteristics	Nanjing cohort ($n = 40$)
Median age at baseline, ng/ml (IQR)	68 (61–75)
Median PSA at baseline, ng/ml (IQR)	17.7 (76.6-383.5)
Metastases site, *n* (%)	
LN	30 (75)
Bone	36 (90)
Visceral	7 (18)
Number of PSMA-positive metastases, *n* (%)	
⩽5	3 (8)
>5	37 (92)
Prior docetaxel treatment, *n* (%)	13 (33)
With ⩾ULK ALP value, *n* (%)	19 (48)

IQR, interquartile range; LN, lymph node; PSA, prostate-specific antigen; PSMA, prostate-specific membrane antigen; ALP, alkaline phosphatase.

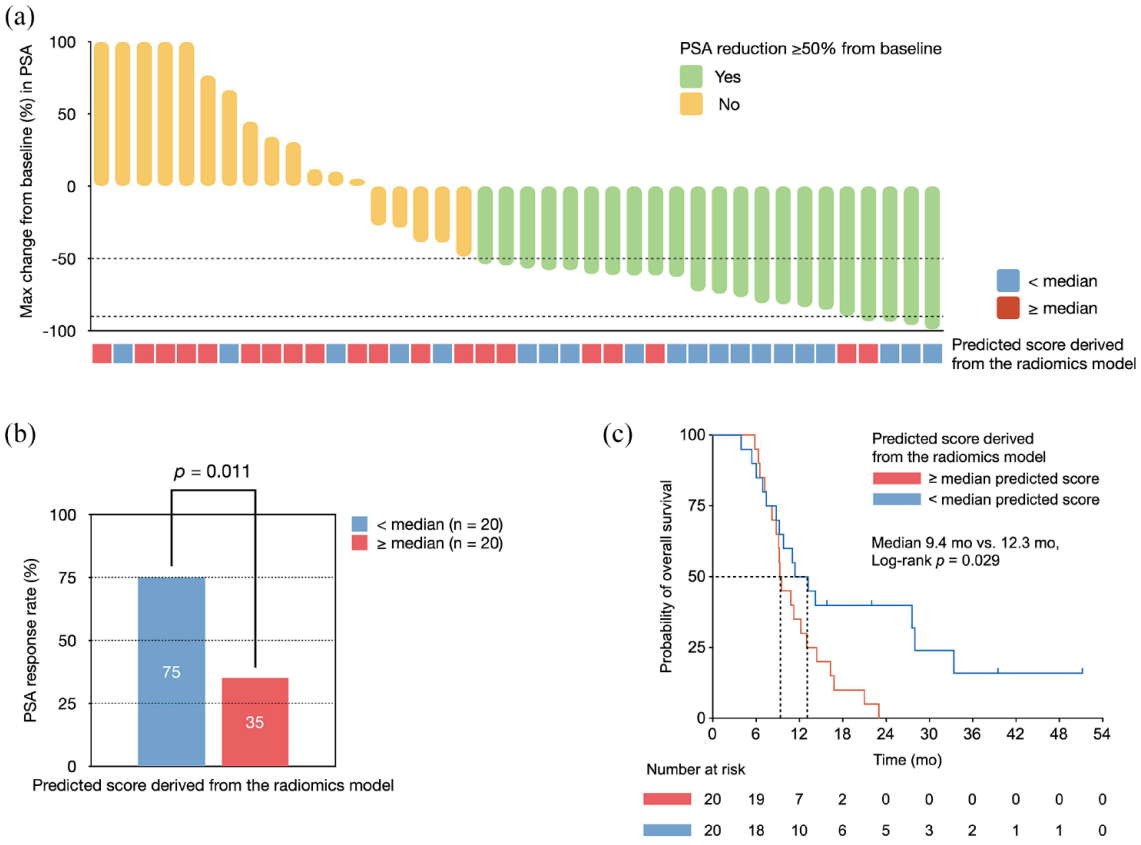

Figure 4. Survival data of the ^{177}Lu-PSMA-617-treated patients with mCRPC from the Nanjing cohort ($n = 40$) stratified by the PSMA−/FDG+ risk according to the radiomics model. (a) Maximal percentage change from baseline in PSA in patients receiving ^{177}Lu-PSMA-617. (b) Impact of predicted score on the PSA response rate. (c) Kaplan–Meier curves for OS according to the predicted score.
FDG, fluorodeoxyglucose; mCRPC, metastatic castration-resistant prostate cancer; OS, overall survival; PSA, prostate-specific antigen; PSMA, prostate-specific membrane antigen.

Our radiomics nomogram, intricately tailored to predict PSMA-/FDG+ disease, found validation in an external cohort where the risk derived from the radiomics model correlated with the PSA response rate and OS after ^{177}Lu-PSMA-617 treatment. These results substantiated the burgeoning body of evidence underscoring the unfavorable outcomes linked to PSMA−/FDG+ lesions.[28] Consequently, it is judicious to contemplate intensifying treatment strategies for patients with a heightened risk of PSMA−/FDG+ lesions, necessitating prospective evidence and precise interventions such as FDG+ tumor ablation or combination treatments.

To the best of our knowledge, this study represents the pioneering effort in generating PSMA−/FDG+ lesions prediction nomograms. Despite the commendable predictive performances of our models, several limitations warrant consideration. First, the retrospective nature of the study introduces the potential for selection bias. Second, the moderate sample size in the development cohort underscores the imperative for prospective validation with a more substantial patient population. However, with the increasing number of ongoing clinical trials (Supplemental Table S4) exploring the integration of ^{177}Lu-PSMA-617 in the front-line setting of mCRPC and oligo-metastatic CRPC, our models may assume a pivotal role in further optimizing individualized care. Lastly, we could not estimate the predictive value of the DNA repair defects [14,29] and the activation of the PI3K-Akt-mTOR pathway,[30,31] factors that may exert influence on the expression of PSMA.

In conclusion, our study culminates in the development of radiomic and clinical nomograms exhibiting promising predictive performances for

PSMA−/FDG+ lesions in CRPC. Patients identified with a heightened risk of PSMA−/FDG+ lesions had a poor prognosis post ^{177}Lu-PSMA-617 treatment. Our models, complemented by online risk calculators, stand poised to contribute significantly to individual medical decision-making and the meticulous design of clinical trials.

Declarations

Ethics approval and consent to participate

This study was approved by the Ethics Committee of Fudan University Shanghai Cancer Center (Ethics Code: 1907204-20) and conducted ethically in accordance with the Declaration of Helsinki in 1964. All patients provided written informed consent.

Consent for publication

Not applicable.

Author contributions

Jian Pan: Conceptualization; Data curation; Formal analysis; Methodology; Writing – original draft; Writing – review & editing.

Tingwei Zhang: Data curation; Methodology; Writing – review & editing.

Shouzhen Chen: Data curation; Formal analysis; Software; Writing – review & editing.

Ting Bu: Formal analysis.

Jinou Zhao: Data curation.

Xudong Ni: Data curation; Methodology; Software.

Benkang Shi: Data curation; Investigation; Software.

Hualei Gan: Data curation; Investigation.

Yu Wei: Data curation; Investigation.

Qifeng Wang: Conceptualization; Data curation; Resources.

Beihe Wang: Data curation; Investigation.

Junlong Wu: Data curation; Investigation.

Shaoli Song: Writing – review & editing.

Feng Wang: Conceptualization; Data curation; Resources.

Chang Liu: Conceptualization; Data curation; Resources.

Dingwei Ye: Conceptualization; Funding acquisition; Resources; Supervision; Writing – review & editing.

Yao Zhu: Conceptualization; Data curation; Formal analysis; Funding acquisition; Methodology; Resources; Writing – original draft; Writing – review & editing.

Acknowledgements

We thank the patients who participated in the studies. And we thank Hongru Shen, Yunhai Pan, Chunxiang Zhang, Runzhi Pan, Qiqi Pan, Rui Shi, Yiyao Huang, Jinghui Wang, Huiru Sun, and Zhijun Zeng, who gave strong support to the present study.

Funding

The authors disclosed receipt of the following financial support for the research, authorship, and/or publication of this article: This study was funded by National Natural Science Foundation of China (81972375, 82172621, and 82203106), Shanghai Anti-Cancer Association Eyas Project (SACA-CY22A04), Shanghai Sailing Program (21YF1408100), Shanghai Medical Innovation Research Special Project (21Y11904300), Shanghai Shenkang Research Physician Innovation and Transformation Ability Training Project (SHDC2022CRD035), Clinical Research Plan of SHDC (SHDC-2020CR2016B), Cancer Research Fund of The Chinese Society of Clinical Oncology (Y-HR2022QN-0532), Clinical Research Project of Shanghai Municipal Health Bureau (20234Y0121), Beijing Xisike Clinical Oncology Research Foundation (Y-2019AZMS-0012 and Y-MSDZD2021-0230), Natural Science Foundation of Shanghai (23ZR1412200), Chinese Anti-Cancer Association Foundation (CETSDHRCORP252-3-018), Shanghai Academic/Technology Research Leader (23XD1420600), Chinese Anti-Cancer Association-Hengrui PARP Inhibitor Cancer Research Foundation, and Oriental Scholar Professorship, Shanghai Municipal Commission of Education, China.

Competing interests

The authors declare that there is no conflict of interest.

Availability of data and materials

Data supporting the findings of this study are available within the supplementary information

and are also available from the authors upon reasonable request.

ORCID iD
Yao Zhu https://orcid.org/0000-0001-7950-6669

Supplemental material
Supplemental material for this article is available online.

References

1. Hofman MS, Emmett L, Sandhu S, *et al.* [(177) lu]lu-psma-617 versus cabazitaxel in patients with metastatic castration-resistant prostate cancer (therap): a randomised, open-label, phase 2 trial. *Lancet* 2021; 397: 797–804.
2. Sartor O, de Bono J, Chi KN, *et al.* Lutetium-177-psma-617 for metastatic castration-resistant prostate cancer. *N Engl J Med* 2021; 385: 1091–1103.
3. Ghezzo S, Bezzi C, Presotto L, *et al.* State of the art of radiomic analysis in the clinical management of prostate cancer: a systematic review. *Crit Rev Oncol Hematol* 2022; 169: 103544.
4. Pan J, Zhao J, Ni X, *et al.* Heterogeneity of [(68) ga]ga-psma-11 pet/ct in metastatic castration-resistant prostate cancer: genomic characteristics and association with abiraterone response. *Eur J Nucl Med Mol Imaging* 2023; 50: 1822–1832.
5. Herrmann K, Kratochwil C, Fendler WP, *et al.* 2021: the year [(177)lu]lu-psma-617 rlt psma is ready for incorporation into clinical guidelines?: Reply to 'a perspective on the eanm procedure guidelines for radionuclide therapy with 177lu-labelled psma-ligands' by dr. Germo gericke. *Eur J Nucl Med Mol Imaging* 2021; 48: 2668–2669.
6. Kumar A, Coleman I, Morrissey C, *et al.* Substantial interindividual and limited intraindividual genomic diversity among tumors from men with metastatic prostate cancer. *Nat Med* 2016; 22: 369–378.
7. Jadvar H. The VISION forward: recognition and implication of PSMA–/(18)F–FDG+ mCRPC. *J Nucl Med* 2021; 63: 812–815.
8. Jadvar H, Ballas LK, Choyke PL, *et al.* Appropriate use criteria for imaging evaluation of biochemical recurrence of prostate cancer after definitive primary treatment. *J Nucl Med* 2020; 61: 552–562.
9. Thang SP, Violet J, Sandhu S, *et al.* Poor outcomes for patients with metastatic castration-resistant prostate cancer with low prostate-specific membrane antigen (psma) expression deemed ineligible for (177)lu-labelled psma radioligand therapy. *Eur Urol Oncol* 2019; 2: 670–676.
10. Lavallee E, Bergeron M, Buteau FA, *et al.* Increased prostate cancer glucose metabolism detected by (18)f-fluorodeoxyglucose positron emission tomography/computed tomography in localised gleason 8-10 prostate cancers identifies very high-risk patients for early recurrence and resistance to castration. *Eur Urol Focus* 2019; 5: 998–1006.
11. Emmett L, Crumbaker M, Ho B, *et al.* Results of a prospective phase 2 pilot trial of (177) lu-psma-617 therapy for metastatic castration-resistant prostate cancer including imaging predictors of treatment response and patterns of progression. *Clin Genitourin Cancer* 2019; 17: 15–22.
12. Jadvar H. Imaging evaluation of prostate cancer with 18f-fluorodeoxyglucose pet/ct: Utility and limitations. *Eur J Nucl Med Mol Imaging* 2013; 40(Suppl 1): S5–S10.
13. Pan J, Wei Y, Zhang T, *et al.* Stereotactic radiotherapy for lesions detected via (68) ga-prostate-specific membrane antigen and (18)f-fluorodexyglucose positron emission tomography/computed tomography in patients with nonmetastatic prostate cancer with early prostate-specific antigen progression on androgen deprivation therapy: A prospective single-center study. *Eur Urol Oncol* 2022; 5: 420–427.
14. Pan J, Zhao J, Ni X, *et al.* The prevalence and prognosis of next-generation therapeutic targets in metastatic castration-resistant prostate cancer. *Mol Oncol* 2022; 16: 4011–4022.
15. Chen R, Wang Y, Zhu Y, *et al.* The added value of (18)f-fdg pet/ct compared to (68)ga-psma pet/ct in patients with castration-resistant prostate cancer. *J Nucl Med* 2022; 63: 69–75.
16. Mottet N, van den Bergh RCN, Briers E, *et al.* Eau-eanm-estro-esur-siog guidelines on prostate cancer-2020 update. Part 1: Screening, diagnosis, and local treatment with curative intent. *Eur Urol* 2021; 79: 243–262.
17. McShane LM, Altman DG, Sauerbrei W, *et al.* Reporting recommendations for tumour marker prognostic studies (remark). *Br J Cancer* 2005; 93: 387–391.
18. Balachandran VP, Gonen M, Smith JJ, *et al.* Nomograms in oncology: more than meets the eye. *Lancet Oncol* 2015; 16: e173–e180.

19. Collins GS, Reitsma JB, Altman DG, *et al.* Transparent reporting of a multivariable prediction model for individual prognosis or diagnosis (tripod). *Ann Intern Med* 2015; 162: 735–736.

20. Bu T, Zhang L, Yu F, *et al.* (177)lu-psma-i&t radioligand therapy for treating metastatic castration-resistant prostate cancer: a single-centre study in east asians. *Front Oncol* 2022; 12: 835956.

21. Gafita A, Calais J, Grogan TR, *et al.* Nomograms to predict outcomes after (177)lu-psma therapy in men with metastatic castration-resistant prostate cancer: an international, multicentre, retrospective study. *Lancet Oncol* 2021; 22: 1115–1125.

22. Fanti S, Briganti A, Emmett L, *et al.* Eau-eanm consensus statements on the role of prostate-specific membrane antigen positron emission tomography/computed tomography in patients with prostate cancer and with respect to [(177)lu]lu-psma radioligand therapy. *Eur Urol Oncol* 2022; 5: 530–536.

23. Gillessen S, Bossi A, Davis ID, *et al.* Management of patients with advanced prostate cancer-metastatic and/or castration-resistant prostate cancer: report of the advanced prostate cancer consensus conference (apccc) 2022. *Eur J Cancer* 2023; 185: 178–215.

24. Michalski K, Ruf J, Goetz C, *et al.* Prognostic implications of dual tracer pet/ct: PSMA ligand and [(18)f]fdg pet/ct in patients undergoing [(177)lu]psma radioligand therapy. *Eur J Nucl Med Mol Imaging* 2021; 48: 2024–2030.

25. Buteau JP, Martin AJ, Emmett L, *et al.* Psma pet and fdg pet as predictors of response and prognosis in a randomized phase 2 trial of 177lu-psma-617 (lupsma) versus cabazitaxel in metastatic, castration-resistant prostate cancer (mcrpc) progressing after docetaxel (therap anzup 1603). *J Clin Oncol* 2022; 40: 10–10.

26. Parker C, Castro E, Fizazi K, *et al.* Prostate cancer: Esmo clinical practice guidelines for diagnosis, treatment and follow-up. *Ann Oncol* 2020; 31: 1119–1134.

27. Sonpavde G, Pond GR, Berry WR, *et al.* Serum alkaline phosphatase changes predict survival independent of PSA changes in men with castration-resistant prostate cancer and bone metastasis receiving chemotherapy. *Urol Oncol* 2012; 30: 607–613.

28. Fox JJ, Gavane SC, Blanc-Autran E, *et al.* Positron emission tomography/computed tomography-based assessments of androgen receptor expression and glycolytic activity as a prognostic biomarker for metastatic castration-resistant prostate cancer. *JAMA Oncol* 2018; 4: 217–224.

29. Paschalis A, Sheehan B, Riisnaes R, *et al.* Prostate-specific membrane antigen heterogeneity and DNA repair defects in prostate cancer. *Eur Urol* 2019; 76: 469–478.

30. Kaittanis C, Andreou C, Hieronymus H, *et al.* Prostate-specific membrane antigen cleavage of vitamin b9 stimulates oncogenic signaling through metabotropic glutamate receptors. *J Exp Med* 2018; 215: 159–175.

31. Zhu Y, Mo M, Wei Y, *et al.* Epidemiology and genomics of prostate cancer in asian men. *Nat Rev Urol* 2021; 18: 282–301.